Response to the comments by Referee 1 and Referee 2.

The response to Referee 1 and Referee 2 follows sequence: (1) comments from Referees, (2) author's response, (3) author's changes in manuscript. The author's changes are marked in blue. In addition, I provide a marked-up manuscript version showing the changes made (using track changes in Word).

I will reply to each comment as follows.

1. To the comments by Referee 1:

Thank you very much for the constructive comments.

I will reply to each comment as follows.

R1-1 ----------

(1) comments from Referee 1

A glance at Figure 2 gives the reassuring impression that random errors are quite small for both the IGS and PRV-HS methods. However, there is a small but significant difference in the results at the one temperature where both techniques are used. This shows a systematic error in one or both of the methods.

(2) author's response

Thank you for the comment. Evaluation of systematic errors or potential systematic bias is also commented by Referee 2. Potential systematic bias of values of K_{eq} determined are estimated to be within ±2% in the IGS method and within ±4% in the PRV-HS method, as described in the revised manuscript.

In the original manuscript, error bars in Fig. 2 represent statics errors (*error_S*) only. I revise Fig. 2 by plotting the data with error bars (*error_T*) representing both *error_S* and potential systematic bias (*error_B*). Values of *error_T* are calculated by (*error_S* + *error_B*) rather than $\sqrt{(error\_S)^2 + (error\_B)^2}$ because *error_B* is potential systematic bias. Tables 1, S1 and 3 list *error_T* as well as *error_S* in the revised manuscript. Fig. 4 is also revised by plotting the data with error bars (*error_T*). Error bars of values of $\frac{F}{k_1 RTV}$ in Figs. 1, 3, S5, S6, S7, and S8 are explained in the captions.

As seen in Fig. 2 in the revised manuscript, potential systematic bias in both the PRV-HS method and the IGS method could be a reason why there is the small offset between PRV-HS and IGS method at 312 K

(3) author's changes in manuscript

lines 13-17, page 5

As described in *Results and discussion* (Sect. 3.1), CH_2F_2 in the headspace over the test solution was not expected to be

redistributed into the test solution. Hence Eq. (6) was used to deduce $K_{eq}(T)$ from k_1. Errors of T are estimated to be within ±0.2 K. These errors of T may give potential systematic bias of ca. ±2% ($\delta K_{eq}/K_{eq}$) where δK_{eq} is error of the value of K_{eq}. Errors of F are estimated to be less than 1.4 %, and theses errors may give potential systematic bias of less than 1.4 % ($\delta K_{eq}/K_{eq}$). Accordingly, for the IGS methods, values of K_{eq} may have potential systematic bias of ca. ±2%.

lines 4-7, page 7

Errors of T are estimated to be within ca. 2 K. These errors of T may give potential systematic bias of ca. ±4% ($\delta K_{eq}/K_{eq}$) at 313 K and ca. ±3% ($\delta K_{eq}/K_{eq}$) at 353 K. Errors of V_0 are estimated to be less than 1 %, and these errors may give potential systematic bias of less than 1 % ($\delta K_{eq}/K_{eq}$). Accordingly, for the PRV-HS methods, values of K_{eq} may have potential systematic bias of ca. ±4%.

lines 3-9, page 8

Figure 2 plots the average K_H values for the V value of 0.350 dm^3 against 100/T. Error bars of the data represent both 2σ for the average and potential systematic bias (±2%). Figure 2 also displays the $K_H(T)$ values obtained by the PRV-HS method. The results of the PRV-HS experiments are described in *Supporting Information* (Fig. S3, Fig. S4 and Table S1). The K_H value obtained by the PRV-HS experiments at each temperature and its error were estimated at 95% confidence level by fitting the two datasets at each temperature (Fig. S4) simultaneously by means of the nonlinear least-squares method with respect to Eq. (11). Error bars of the data by PRV-HS method in Fig. 2 represent both errors at 95% confidence level for the regression and potential systematic bias (±4%).

Caption, Fig. 1

Plots of values of $F/(k_1RTV)$ against F at each temperature for 0.350 dm^3 and 0.300 dm^3 of deionized water. Error bars represent 2σ due to errors of values of k_1 as described in Sect. S2 in Supporting Information. Grey symbols represent the data excluded for calculating the average.

Caption, Fig. 3

Plots of values of $F/(k_1RTV)$ against F at each temperature for 0.35 dm^3 of a-seawater at 36.074‰. Grey symbols represent the data excluded for calculating the average. Error bars represent 2σ due to errors of values of k_1 as described in Sect. S2 in Supporting Information. Grey symbols represent the data excluded for calculating the average.

Caption, Fig. S5

Plots of values of $F/(k_1RTV)$ against F at each temperature for 0.35 dm^3 of a-seawater at 4.452‰. Error bars represent 2σ due to errors of values of k_1 as described in Sect. S2. Grey symbols represent the data excluded for calculating the average.

Caption, Fig. S6

Plots of values of $F/(k_1RTV)$ against F at each temperature for 0.35 dm^3 of a-seawater at 8.921‰. Error bars represent 2σ due to errors of values of k_1 as described in Sect. S2. Grey symbols represent the data excluded for calculating the average.

Caption, Fig. S7

Plots of values of $F/(k_1RTV)$ against F at each temperature for 0.35 dm^3 of a-seawater at 21.520‰. Error bars represent 2σ due to errors of values of k_1 as described in Sect. S2. Grey symbols represent the data excluded for calculating the average.

Caption, Fig. S8

Plots of values of $F/(k_1RTV)$ against F at each temperature for 0.35 dm^3 of a-seawater at 51.534‰. Error bars represent 2σ due to errors of values of k_1 as described in Sect. S2. Grey symbols represent the data excluded for calculating the average.

Fig. 2

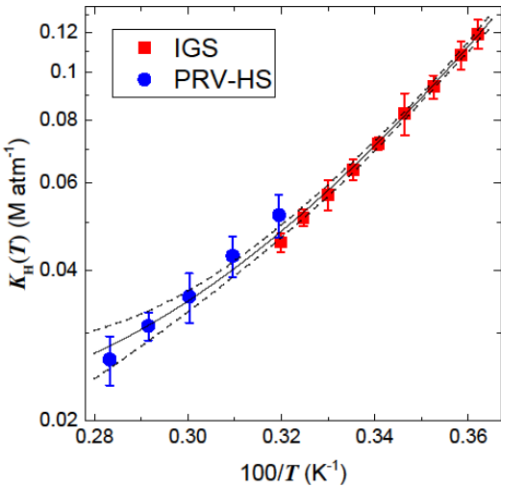

Figure 2. van't Hoff plot of the K_H values obtained by the IGS method and the PRV-HS method. Bold curve displays the fitting of the data obtained by the IGS method and the PRV-HS method (Eq. (13)). Dashed curves display upper and lower 95% confidence limit of the above fitting by Eq. (12). Error bars of the data by the IGS method represent both 2σ for the average and potential systematic bias. Error bars of the data by PRV-HS method represent both errors at 95% confidence level for the regression and potential systematic bias.

Fig. 4

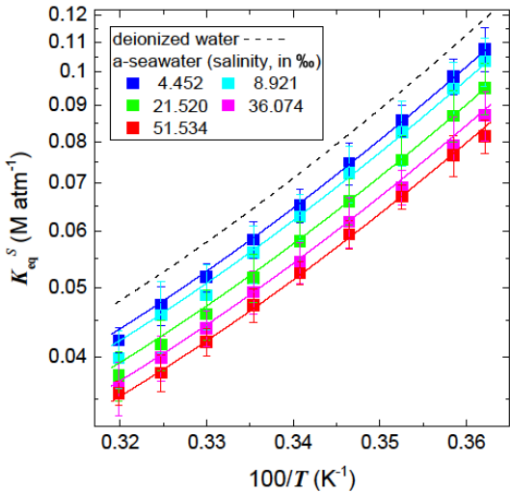

Figure 4. van't Hoff plot of the K_{eq}^{S} values for a-seawater at each salinity. Dashed curve represents the K_H values by Eq. (13). Bold curves represent the fitting obtained by Eq. (23). Error bars of the data represent both 2σ for the average and potential systematic bias.

Table 1

Table 1. The average of values of $F/(k_1RTV)$ obtained for V value of 0.350 dm^3 and 0.300 dm^3 and the $K_H(T)$ value derived from Eq. (13) at each temperature. N represents number of experimental runs for the average.

T (K)	F / (k_1RTV)				$K_H(T)$ (M atm^{-1})
	V = 0.350		V = 0.300		
	average [a, b]	N [c]	average [a]	N [c]	From Eq. (13) [d, e]
276.15	0.119 ± 0.006 (0.008)	21 (2)	0.117 ± 0.006 (0.008)	11 (0)	0.118 ± 0.003 (0.005)
278.35	0.107 ± 0.005 (0.007)	18 (3)	0.110 ± 0.005 (0.007)	14 (0)	0.108 ± 0.002 (0.004)
283.65	0.093 ± 0.003 (0.005)	27 (5)	0.092 ± 0.001 (0.003)	5 (0)	0.094 ± 0.002 (0.004)
288.65	0.082 ± 0.006 (0.008)	41 (5)	0.084 ± 0.006 (0.008)	12 (0)	0.082 ± 0.002 (0.004)
293.45	0.071 ± 0.001 (0.002)	15 (8)	0.071 ± 0.001 (0.002)	5 (0)	0.072 ± 0.002 (0.003)
298.15	0.064 ± 0.002 (0.003)	30 (6)	0.067 ± 0.005 (0.006)	12 (0)	0.064 ± 0.002 (0.003)
303.05	0.057 ± 0.003 (0.004)	16 (0)	0.056 ± 0.005 (0.006)	4 (0)	0.058 ± 0.002 (0.003)
307.95	0.051 ± 0.001 (0.002)	12 (6)	0.054 ± 0.004 (0.005)	10 (0)	0.052 ± 0.002 (0.003)
312.65	0.046 ± 0.001 (0.002)	13 (3)	0.047 ± 0.001 (0.002)	4 (0)	0.048 ± 0.001 (0.002)

a. Errors are 2σ for the average only.; b. Number in parenthesis represents an error reflecting both 2σ for the average and potential systematic bias (±2%).; c. Number in parenthesis represents number of experimental runs excluded for the average.; d. Errors are 95% confidence level for the regression only.; e. Number in parenthesis represents an error reflecting both errors at 95% confidence level for the regression and potential systematic bias (±2%).

Table S1

Table S1. L_i values for various V_i/V_0 ratios at various temperatures, slopes and intercepts for linear regression with respect to Eq. (10), $K_H(T)$ values calculated from the slopes and intercepts, and $K_H(T)$ values and the errors at 95% confidence level estimated by non-linear fitting the two datasets simultaneously at each temperature (Fig. S4) with respect to Eq. (11).

T (K)	L_i (a.u.) [a]						Eq. (10) Intercept	Eq. (10) Slope	K_H (M atm^{-1})		
	V_i/V = 0.421	0.351	0.280	0.210	0.140	0.070			Eq. (10)	Eq. (11) [b, c]	Eq. (13) [b]
353	3.226±0.002	3.270±0.026	3.330±0.004	3.391±0.008	3.462±0.014	3.526±0.009	3.581	–0.870	0.026	0.027 ±0.002 (±0.003)	0.031 ±0.003
	2.044±0.006	2.050±0.012	2.112±0.010	2.132±0.009	2.186±0.021	2.209±0.011	2.248	–0.513	0.027		
343	3.000±0.018	3.025±0.009	3.070±0.008	3.089±0.015	3.117±0.015	3.148±0.018	3.179	–0.423	0.031	0.031 ±0.001 (±0.002)	0.033 ±0.002
	1.949±0.004	1.955±0.005	1.968±0.003	1.998±0.004	2.020±0.002	2.030±0.009	2.050	–0.258	0.031		
333	3.247±0.018	3.234±0.018	3.243±0.015	3.241±0.010	3.247±0.009	3.223±0.013	3.231	0.034	0.037	0.036 ±0.003 (±0.004)	0.037 ±0.002
	3.080±0.009	3.044±0.006	3.082±0.005	3.127±0.009	3.113±0.008	3.134±0.014	3.149	–0.213	0.034		
323	3.208±0.011	3.190±0.008	3.133±0.010	3.134±0.011	3.092±0.008	3.093±0.006	3.055	0.355	0.042	0.043 ±0.002 (±0.004)	0.042 ±0.001
	3.357±0.010	3.289±0.014	3.275±0.005	3.233±0.004	3.226±0.016	3.160±0.001	3.135	0.496	0.044		
313	3.245±0.018	3.185±0.013	3.100±0.015	3.022±0.012	2.995±0.012	2.915±0.011	2.848	0.935	0.052	0.052 ±0.003 (±0.005)	0.049 ±0.001
	2.162±0.031	2.134±0.010	2.060±0.014	2.029±0.018	1.992±0.010	1.925±0.018	1.896	0.612	0.052		

a. Errors are 2σ for the regression only.; b. Errors are those at 95% confidence level for the regression only.; c. Number in parenthesis represents both errors at 95% confidence level for the regression and potential systematic bias (±4%).

Table 3

Table 3. The average of values of $F/(k_1RTV)$ obtained for V value of 0.350 dm^3 and the $K_{eq}^{S}(T)$ value derived from Eq. (23) at each salinity and temperature. N represents number of experimental runs for the average.

T (K)	K_{eq}^{S} (M atm^{-1})					
	salinity, 4.452 ‰			salinity, 8.921 ‰		
	average [a, b]	N [c]	Eq. (23) [d, e]	average [a, b]	N [c]	Eq. (23) [d, e]
276.15	0.108 ± 0.006 (0.008)	8 (0)	0.107 ± 0.003 (0.005)	0.103 ± 0.006 (0.008)	21 (0)	0.102 ± 0.003 (0.005)
278.35	0.099 ± 0.004 (0.006)	12 (0)	0.098 ± 0.002 (0.005)	0.095 ± 0.006 (0.008)	26 (1)	0.094 ± 0.002 (0.004)
283.65	0.086 ± 0.003 (0.005)	9 (0)	0.085 ± 0.002 (0.004)	0.083 ± 0.007 (0.009)	24 (0)	0.081 ± 0.002 (0.004)
288.65	0.075 ± 0.004 (0.006)	12 (0)	0.074 ± 0.002 (0.003)	0.072 ± 0.005 (0.006)	33 (0)	0.071 ± 0.001 (0.002)
293.45	0.065 ± 0.002 (0.003)	10 (0)	0.065 ± 0.002 (0.003)	0.063 ± 0.003 (0.004)	27 (5)	0.063 ± 0.002 (0.003)
298.15	0.058 ± 0.002 (0.003)	13 (0)	0.058 ± 0.002 (0.003)	0.056 ± 0.004 (0.005)	26 (2)	0.056 ± 0.002 (0.003)
303.05	0.052 ± 0.001 (0.002)	8 (0)	0.052 ± 0.002 (0.003)	0.049 ± 0.004 (0.005)	14 (6)	0.050 ± 0.001 (0.002)
307.95	0.047 ± 0.002 (0.003)	13 (1)	0.048 ± 0.001 (0.002)	0.046 ± 0.004 (0.005)	23 (1)	0.046 ± 0.001 (0.002)
312.65	0.042 ± 0.001 (0.002)	7 (0)	0.044 ± 0.001 (0.002)	0.040 ± 0.003 (0.004)	12 (8)	0.042 ± 0.001 (0.002)

T (K)	K_{eq}^{S} (M atm^{-1})					
	salinity, 21.520 ‰			salinity, 36.074 ‰		
	average [a, b]	N [c]	Eq. (23) [d, e]	average [a, b]	N [c]	Eq. (23) [d, e]
276.15	0.095 ± 0.006 (0.008)	20 (0)	0.094 ± 0.003 (0.005)	0.088 ± 0.005 (0.007)	21 (0)	0.088 ± 0.002 (0.004)
278.35	0.087 ± 0.005 (0.007)	22 (0)	0.086 ± 0.002 (0.004)	0.079 ± 0.006 (0.008)	20 (3)	0.081 ± 0.002 (0.004)
283.65	0.075 ± 0.004 (0.006)	15 (1)	0.075 ± 0.001 (0.003)	0.069 ± 0.002 (0.003)	18 (2)	0.070 ± 0.001 (0.002)
288.65	0.066 ± 0.004 (0.005)	20 (0)	0.066 ± 0.001 (0.002)	0.062 ± 0.004 (0.005)	19 (4)	0.061 ± 0.001 (0.002)
293.45	0.058 ± 0.003 (0.004)	14 (0)	0.058 ± 0.001 (0.002)	0.054 ± 0.002 (0.003)	19 (4)	0.055 ± 0.001 (0.002)
298.15	0.052 ± 0.003 (0.004)	20 (0)	0.052 ± 0.001 (0.002)	0.049 ± 0.002 (0.003)	24 (4)	0.049 ± 0.001 (0.002)
303.05	0.046 ± 0.003 (0.004)	16 (0)	0.047 ± 0.001 (0.002)	0.044 ± 0.002 (0.003)	16 (0)	0.044 ± 0.001 (0.002)
307.95	0.042 ± 0.003 (0.004)	16 (0)	0.042 ± 0.001 (0.002)	0.040 ± 0.002 (0.003)	15 (2)	0.040 ± 0.001 (0.002)
312.65	0.038 ± 0.002 (0.003)	16 (0)	0.039 ± 0.001 (0.002)	0.036 ± 0.002 (0.003)	16 (0)	0.037 ± 0.001 (0.002)

T (K)	K_{eq}^{S} (M atm^{-1})		
	salinity, 51.534 ‰		
	average [a, b]	N [c]	Eq. (23) [d, e]
276.15	0.081 ± 0.003 (0.005)	10 (0)	0.083 ± 0.002 (0.004)
278.35	0.077 ± 0.003 (0.005)	15 (0)	0.076 ± 0.002 (0.004)
283.65	0.067 ± 0.001 (0.003)	9 (1)	0.067 ± 0.001 (0.002)
288.65	0.059 ± 0.002 (0.003)	14 (1)	0.058 ± 0.001 (0.002)
293.45	0.052 ± 0.001 (0.002)	7 (3)	0.052 ± 0.001 (0.002)
298.15	0.047 ± 0.002 (0.003)	15 (0)	0.046 ± 0.001 (0.002)
303.05	0.042 ± 0.001 (0.002)	8 (0)	0.042 ± 0.001 (0.002)
307.95	0.038 ± 0.002 (0.003)	12 (0)	0.038 ± 0.001 (0.002)
312.65	0.036 ± 0.001 (0.002)	7 (1)	0.035 ± 0.001 (0.002)

a. Errors are 2σ for the average only.; b. Number in parenthesis represents an error reflecting both 2σ for the average and potential systematic bias.; c. Number in parenthesis represents number of experimental runs excluded for the average.; d. Errors are 95% confidence level for the regression only.; e. Number in parenthesis represents an error reflecting both errors at 95% confidence level for the regression and potential systematic bias (±2%).

R1-2 ----------

(1) comments from Referee 1

In the fitting equation, equation 13, the number of significant figures reported is much higher than justified for the relatively small number of data points. In nonlinear fitting of this type, most programs report the variance associated with each of the fitting coefficients. If the square-root-of-variance is not small compared to the fitting coefficient, that means that the inclusion of that coefficient is probably not justified.

(2) author's response

Thank you for the comments. According to Referee 1's comment, I revise the significant figure of each fitting coefficient in Eq. (13). I set the least digit of the significant figure to the second decimal place so that the values calculated by Eq. (13) are consistent with the significant figure of K_H.

Thank you for the suggestion that the square-root-of-variance of the fitting coefficient should be checked for justifying whether the coefficient should be included in the van't Hoff equation.

The square-root-of-variance, that is, standard deviation for each fitting coefficient in Eq. (12) justifies the three-term van't Hoff equation. The standard deviation for each fitting coefficient is described in the revised manuscript. Because the ratio of $2\times\delta a_3/a_3$ is 0.293, the three-term van't Hoff equation is thus justified.

In addition, even if the data only in the IGS method is fitted separately, a three-term fit to the data in the IGS method would be justified as Eq. (A1), although errors of the fitting coefficients are larger than those in Eq. (13).

$$\ln(K_H(T)) = (-41.7 \pm 7.2) + (66.8 \pm 10.5) \times \left(\frac{100}{T}\right) + (15.1 \pm 3.7) \times \ln\left(\frac{T}{100}\right) \quad \text{(A1)}$$

where errors of the fitting coefficients represent standard deviation only for non-linear fitting.

(3) author's changes in manuscript

<u>lines 14-16, page 8</u>

$$\ln\left(K_H(T)\right) = -49.71 + 77.70 \times \left(\frac{100}{T}\right) + 19.14 \times \ln\left(\frac{T}{100}\right) \quad (13).$$

The square-root-of-variance, that is, standard deviation for each fitting coefficient in Eq. (12) is as follows:

$\delta a_1 = 5.5$; $\delta a_2 = 8.3$; $\delta a_3 = 2.8$.

R1-3 ----------

(1) comments from Referee 1

The treatment of the salting-out effect is overworked. In Referee 1's opinion, lines 9-26, page 9 should be eliminated and the author should simply state that $\ln(K_H/K_{eq})$ varies close to the 0.5 power of salinity, in contrast to the Sechenow.

(2) author's response

Thank you for the constructive comments. I agree the comment that the treatment of the salting-out effect is overworked. I followed the referee's opinion and found that all the data in Fig. 5 could be fitted using only one parameter (Eq. (22)) as described in the revised manuscript.

In the revised manuscript, error bars in Fig. 5 reflect error_T (R1-1) and Figs. 4 (shown in R1-2) and 6 are redrawn according to Eq. (23).

(3) author's changes in manuscript

lines 10-12, page 1, Abstract

The salinity dependence of K_{eq}^{S} (the salting-out effect), $\ln(K_H/K_{eq}^{S})$, did not obey the Setchenow equation but was proportional to $S^{0.5}$. Overall, the $K_{eq}^{S}(T)$ value was expressed by $\ln(K_{eq}^{S}(T)) = -49.71 + (77.70 - 0.134 \times S^{0.5}) \times (100/T) + 19.14 \times \ln(T/100)$.

lines 2-17, page 10

This result suggests that $\ln(K_H(T)/K_{eq}^{S}(T))$ varied according to Eq. (18):

$$\ln(K_H(T)/K_{eq}^{S}(T)) = k_{s1} S^{0.5} \quad (18)$$

Values of k_{s1} may be represented by the following function of T:

$$k_{s1} = b_1 + b_2 \times (100/T) \quad (19)$$

Parameterizations of b_1 and b_2 obtained by fitting all the $\ln(K_H(T)/K_{eq}^{S}(T))$ and S data at each temperature simultaneously by means of the nonlinear least-squares method gives Eq. (20).

$$\ln(K_H(T)/K_{eq}^{S}(T)) = (0.0127 + 0.0099 \times (100/T)) \times S^{0.5} \quad (20)$$

The standard deviation for each fitting coefficient in Eq. (19) is as follows:

$\delta b_1 = 0.0106$; $\delta b_2 = 0.0031$.

Since $2 \times \delta b_1 > b_1$, the parameterization by Eq. (19) may be overworked. Accordingly, all the $\ln(K_H(T)/K_{eq}^{S}(T))$ and S data at each temperature are fitted simultaneously using Eq. (21) instead of Eq. (19). The nonlinear least-squares method gives Eq. (22).

$$k_{s1} = b_2 \times (100/T) \quad (21)$$

$$\ln(K_H(T)/K_{eq}^{S}(T)) = 0.1343 \times (100/T) \times S^{0.5} \quad (22)$$

The standard deviation for the fitting coefficient in Eq. (21) is as follows: $\delta b_2 = 0.0013$. As seen in Fig. 5, Eqs. (21) and (22) reproduced the data well.

lines 26-27, page 10

In Eq. (22), $K_H(T)$ is represented by Eq. (13), as described in Sect. 3.1. Therefore ${K_{eq}}^S(T)$ is represented by Eq. (23):.

$$\ln\left({K_{eq}}^S\right) = -49.71 + (77.70 - 0.1343 \times S^{0.5}) \times \left(\frac{100}{T}\right) + 19.14 \times \ln\left(\frac{T}{100}\right) \quad (23)$$

Fig 6

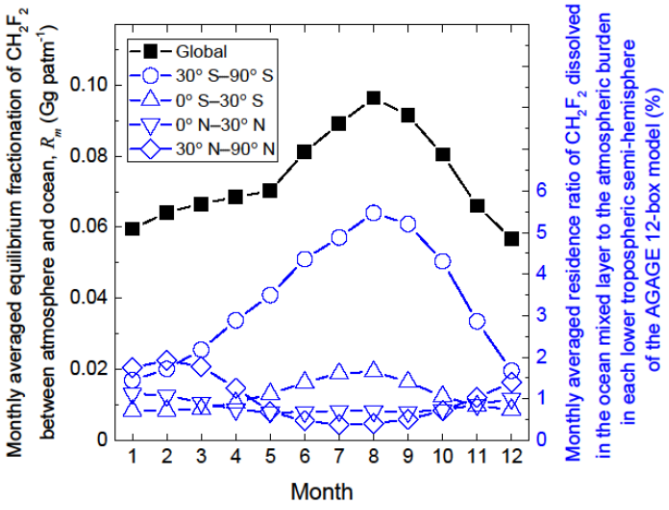

Figure 6. Plots of monthly averaged equilibrium fractionation of CH_2F_2 between atmosphere and ocean, R_m (Gg patm^{-1}) in the global and the hemispheric atmosphere. Right vertical axis represents monthly averaged residence ratio of CH_2F_2 dissolved in the ocean mixed layer to the atmospheric burden for each lower tropospheric semi-hemisphere of the AGAGE 12-box model.

R1-4 ----------

(1) comments from Referee 1

On page 3, lines11-12 (in the revised manuscript), the water quality should be indicated as (resistivity > 18 megohm-cm).

(2) author's response

Thank you for the comment. I correct the text according to the comment.

(3) author's changes in manuscript

lines 11-12, page 3

Water was purified with a Milli-Q Gradient A10 system (resistivity > 18 megohm-cm).

R1-5 ----------

(1) comment from Referee 1

On page 7, line 1 (in the revised manuscript), "non-linear" is misspelled.

(2) author's response

Thank you for the comment. I correct the text according to the comment.

(3) author's changes in manuscript

lines 1-2, page 7

Furthermore, values of $K_{eq}(T)$ and errors of them were determined by non-linear fitting of the data of L_i and V_i/V by means of Eq. (11), which was obtained from Eq. (10):

2. To the comments by Referee 2:

Thank you very much for the constructive comments.

I will reply to each comment as follows.

R2-1 ----------

(1) comments from Referee 2

The manuscript would benefit from an explicit discussion of experimental error. What are the parameters that limit the accuracy of the inert-gas stripping (IGS) method? Of the stripping column apparatus? And of the phase ratio variation headspace method (PRV-HS)? Do error bars reflect statics only, or also potential sources of systematic bias?

(2) author's response

Thank you for the comment. I reply to the comments in the sequence: (i) on the parameters that limit the accuracy of the IGS method; (ii) on the parameters that limit the accuracy of the PRV-HS method; and (ii) on error bars.

(i) the parameters that limit the accuracy of the IGS methods

The parameters that limit the accuracy of the IGS methods are temperature of the test solution (*T*) and flow

rate of purge gas (F).

The accuracy of T (δT) are within 0.2 K and may give potential systematic bias of ±0.5 to ±0.6 % ($\delta K_{eq}/K_{eq}$), where δK_{eq} indicates an error of K_{eq}.

For F, the accuracy of F_{meas} is estimated to be within 1% from the accuracy of the high-precision film flow meter SF-1U with VP-2U used for calibrating the soap flow meter. Errors in the term of $\frac{P_{meas}-h_{meas}}{P_{hs}-h} \times \frac{T}{T_{meas}}$ in Eq (3) are estimated at ca. ±1 %. Hence, the accuracy of F (δF) are estimated to be within 1.4 % and may give potential systematic bias of ±1.4 % of $\delta K_{eq}/K_{eq}$.

Values of $\delta K_{eq}/K_{eq}$ due to both δT and δF may thus have potential systematic bias of ca. ±2%.

(ii) the parameters that limit the accuracy of the PRV-HS methods

The parameters that limit the accuracy of the PRV-HS methods are temperature of the test solution (T) and volume of the vials used (V).

Although the apparatus used (Agilent, HP7694) was expected to keep T constant, the accuracy of T may not be certified. I have applied the same apparatus to determination of the K_H values for some HCFCs such as HCFC-123 using the PRV-HS methods [Kutsuna, S. *Int. J. Chem. Kinet.*, 45, 440-451, 2013]. On the basis of the K_H values thus determined and comparison between them and the reported values for HCFC-123, errors of T are estimated to be within ca. 2 K. These errors of T may give potential systematic bias of ca. ±4 % ($\delta K_{eq}/K_{eq}$) at 313 K and ca. ±3 % ($\delta K_{eq}/K_{eq}$) at 353 K.

Errors for V (δV) are estimated to be less than 1 %, and these errors may give potential systematic bias of less than 1 % of $\delta K_{eq}/K_{eq}$.

Accordingly, for the PRV-HS methods, values of $\delta K_{eq}/K_{eq}$ due to both δT and δV may have potential systematic bias of ca. ±4%.

(iii) Error bars in Figure 2

Error bars in Figure 2 reflect statics only (error_S) in the original manuscript. Error bars in Figure 2m represent errors (error_T) reflecting both error_S and potential systematic bias (error_B). Values of error_T are also indicated in Tables 1m, S1m and 3m. Values of error_T are calculated by (error_S + error_B) rather than $\sqrt{(\text{error\_S})^2 + (\text{error\_B})^2}$ because error_B is potential systematic bias.

(3) author's changes in manuscript

The change in manuscript is the same as described in R1-1.

R2-2 ----------

(1) comments from Referee 2

There does appear to be a small -yet significant- offset between PRV-HS and IGS method in Figure 2. Why IGS is believed to be more accurate?

(2) author's response

Thank you for the comment. There appears to be a small - yet significant - offset between PRV-HS and IGS method at 312 K. This point is also commented by Referee 1. For the PRV-HS methods, values of $\delta K_{eq}/K_{eq}$ may have potential systematic bias of ca. ±4%, which results mostly from the accuracy of temperature of the test solution, as aforementioned (R2-1). For the IGS method, values of $\delta K_{eq}/K_{eq}$ may have potential systematic bias of ca. ±2%. The IGS method is thus believed to be more accurate. Potential systematic bias in both the PRV-HS method and the IGS method could be a reason why there is the small offset between PRV-HS and IGS method at 312 K.

(3) author's changes in manuscript

The change in manuscript related to this comment is included in the changes described in R1-1.

R2-3 ----------

(1) comments from Referee 2

Does the fit according to (Eq (13)) take into account the relative weight of error bars?

(2) author's response

Thank you for the comment. The fit according to Eq. (13) does not take into account the relative weight of error bars. This is clearly described in the revised manuscript.

(3) author's changes in manuscript

lines 10-11, page 8:

All the K_H values were regressed with respect to the van't Hoff equation (Eq. (12)) with no weighting (Clarke and Glew, 1965; Weiss, 1970):

R2-4 ----------

(1) comments from Referee 2

What is the reason for the large variation in the size of error bars in Fig. 5?

(2) author's response

Thank you for the comment. As Referee 2 comments, there are the large variation in the size of error bars in Fig. 5. Ratio among error bars of the data at the same temperature is up to maximum value of 4.5: error bars are 0.084 for 8.921‰ and 0.019 for 51.534‰ at 10.5 °C. Error bars for the data at 8.921‰ tend to be large and error bars for the data at 51.534‰ tend to be small: this reflects statics errors of the data at 8.921‰ and 51.534‰.

Errors of the data in Fig. 5 represents statics only (error_S, as shown in R2-1). As replied in R2-1, errors from both statics (error_S) and potential systematic bias of ±2% (error_B) will be used as errors (error_T) for the data in Fig. 5: (error_T) = (error_S) + (error_B). In the revised manuscript, error bars of the data in Fig. 5 represent error_T. As seen in Fig. 5 in the revised manuscript, the ratios among error bars of the data at the same temperature are smaller than the corresponding ratios in Fig. 5 in the original manuscript. For example, the ratio of error bars between at 8.921‰ and 51.534‰ at 10.5 °C is 2.7 while it is 4.5 in the original manuscript as aforementioned.

In the revised manuscript, error bars will be represented by error_T in Fig. 5.

(3) author's changes in manuscript

Figure 5:

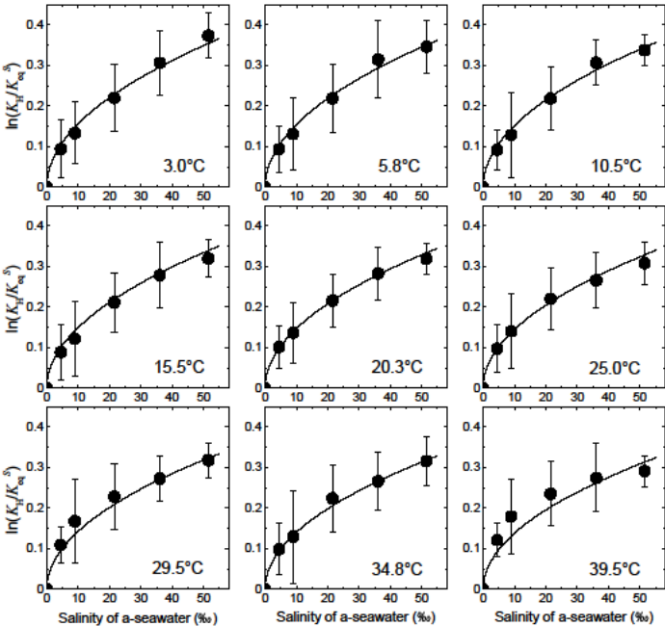

Figure 5. Plots of $\ln(K_H(T)/K_H^S(T))$ vs. salinity in a-seawater at each temperature. Bold curves represent the fitting obtained by Eq. (22). Error bars represent errors reflecting both 2σ for the average and potential systematic bias (2%) of K_{eq}^S.

R2-5 ----------

(1) comments from Referee 2

The $S^{0.5}$ components of the fit (deviation from Setchenow) is strongest at warm temperatures, and smallest at low temperatures. This is an interesting observation, that warrants diiscussion. What are possible causes? What is its relevance?

(2) author's response

Thank you for the comment. The reason why $\ln(K_H/K_{eq}^{S})$ is proportional to $S^{0.5}$ rather than S is still unclear. I will describe a potential reason for this proportionality simply in the text, and make discussion in *Supporting Information*.

(3) author's changes in manuscript

lines 22-25, page 10:

The reason for this salting-out effect of CH_2F_2 solubility in a-seawater is not clear. Specific properties of CH_2F_2 –small molecular volume, which results in small work of cavity creation (Graziano, 2004; 2008), and large solute-solvent attractive potential energy in water and a-seawater− may cause deviation from Setchenow relationship (Sect. S5, *Supporting Information*).

Sect. S5 (pages 7-8) in Supporting Information:

I calculate Ben-Naim standard Gibbs energy $\Delta G^{\cdot}$, enthalpy $\Delta H^{\cdot}$, and entropy $\Delta S^{\cdot}$ changes for dissolution of CH_2F_2 in water because these values correspond to the values for the transfer from a fixed position in the gas phase to a fixed position in water. Values of $\Delta G^{\cdot}$, $\Delta H^{\cdot}$, and $\Delta S^{\cdot}$ are calculated on the basis of the Ostwald solubility coefficient, $L(T)$, as follows.

$$\ln(L(T)) = \ln\left(RTK_{eq}^{S}(T)\right) \quad \text{(B1)}$$

$$\Delta G^{\cdot} = R'T\ln(L(T)) \quad \text{(B2)}$$

$$\Delta H^{\cdot} = -\frac{\partial}{\partial(1/T)}\left(\frac{\Delta G^{\cdot}}{T}\right) \quad \text{(B3)}$$

$$\Delta S^{\cdot} = \frac{\Delta H^{\cdot} - \Delta G^{\cdot}}{T} \quad \text{(B4)}$$

where both R and R' represent gas constant but their units are different: R = 0.0821 in atm dm^3 K^{-1} mol^{-1}; R' = 8.314 in J K^{-1} mol^{-1}.

Combining Eqs. (B1), (B2), (B3), and (B4) with Eqs. (14) and (15), $\Delta G^{\cdot}$ (kJ mol^{-1}), $\Delta H^{\cdot}$ (kJ mol^{-1}), and $\Delta S^{\cdot}$ (J mol^{-1} K^{-1}) are represented by ΔG_{sol} and ΔH_{sol} as follows:

$$\Delta G^{\cdot} = \Delta G_{sol} + R'T\ln(RT) \quad \text{(B5)}$$

$$\Delta H^{\cdot} = \Delta H_{sol} + R'T \quad \text{(B6)}$$

$$\Delta S^{\cdot} = \frac{\Delta H_{sol} - \Delta G_{sol}}{T} + R'T - R'T\ln(RT) \quad \text{(B7)}$$

Values of $\Delta G^{\cdot}$, $\Delta H^{\cdot}$, and $\Delta S^{\cdot}$ calculated at 298 K are listed in Table S2. Table S2 also lists values of $\Delta G^{\cdot}$, $\Delta H^{\cdot}$, and $\Delta S^{\cdot}$ reported for CH_3F and C_2H_6 (Graziano, 2004) and CH_4 (Graziano, 2008) at 298 K. The chemicals, which having a methyl group, in Table S2 are classified into two groups (CH_2F_2 and CH_3F; CH_4 and C_2H_6) according to $\Delta G^{\cdot}$.

Table S2 lists values of ΔG_c, E_a and ΔH^h deduced using a scaled particle theory (Granziano, 2004; 2008). ΔG_c is the work of cavity creation to insert a solute in a solvent. E_a is a solute-solvent attractive potential energy and accounts for the solute-solvent interactions consisting of dispersion, dipole-induced dipole, and dipole-dipole contributions. ΔH^h is enthalpy of solvent molecules reorganization caused by solute insertion. The solvent reorganization mainly involves a rearrangement of H-bonds.

ΔG_c is entropic in nature in all liquids, being a measure of the excluded volume effect due to a reduction in the spatial configurations accessible to liquid molecules upon cavity creation. Hence, C_2H_6 has larger value of ΔG_c than CH_3F and CH_4. ΔG_c, E_a, and ΔH^h are related to $\Delta G^{\cdot}$ and $\Delta H^{\cdot}$ as follows (Graziano, 2008):

$$\Delta G^{\cdot} = \Delta G_c + E_a \quad \text{(B8)}$$

$$\Delta H^{\cdot} = E_a + \Delta H^h \quad \text{(B9)}$$

Table S3 thus suggests that smaller value of $\Delta G^{\cdot}$ of CH_3F than CH_4 is due to large solute-solvent attractive potential energy ($-E_a$) of CH_3F.

Table S3. Ben-Naim standard hydration Gibbs energy $\Delta G^{\cdot}$, enthalpy $\Delta H^{\cdot}$, and entropy $\Delta S^{\cdot}$ changes for dissolution of CH_2F_2 at 298 K determined here and the corresponding values and values of ΔG_c, E_a and ΔH^h reported for CH_3F and C_2H_6 (Granziano, 2004) and CH_4 (Graziano, 2008).

	$\Delta G^{\cdot}$ (kJ mol^{-1})	$\Delta H^{\cdot}$ (kJ mol^{-1})	$\Delta S^{\cdot}$ (J K^{-1} mol^{-1})	ΔG_c (kJ mol^{-1})	E_a (kJ mol^{-1})	ΔH^h (kJ mol^{-1})
CH_2F_2	−1.1	−14.7	−45.4			
CH_3F	−0.9	−15.8	−50.0	23.3	−24.3	8.5
CH_4	8.4	−10.9	−64.7	22.9	−14.5	3.7
C_2H_6	7.7	−17.5	−84.5	28.4	−20.7	3.2

Graziano (2008) definitively explained the salting-out of CH_4 by sodium chloride at molecular level on the basis of a scaled particle theory. He explained that $\Delta G^{\cdot}$ increase was linearly related to the increase in the volume packing density of the solutions (ξ_3) with adding NaCl. Such a increase of $\Delta G^{\cdot}$ is probably the case for salting-out of CH_2F_2 by a-seawater observed in this study. He also explained that E_a was linearly related to the increase in ξ_3 assuming that a fraction of the dipole-induced dipole attractions could be taken into account by the parameterization of the dispersion contribution.

I think the possibility that E_a may be nonlinearly related to the increase in ξ_3 because of dipole-dipole interaction between CH_2F_2 and solvents. Temperature dependence in Eq. (22) suggests that salting-out effect of CH_2F_2 by a-seawater is enthalpic. Eqs. (22) and (B9) thus suggests that the salting-out of CH_2F_2 is mostly related to change in E_a. CH_2F_2 has relatively small value of ΔG_c because of its small molecular volume compared to other chemicals such as C_2H_6. Accordingly,

ΔG^*, that is, solubility of CH_2F_2 would depend on E_a rather than ΔG_c. Therefore, I think that specific properties of CH_2F_2 – small molecular volume, which results in small work of cavity creation (Graziano, 2004; 2008), and large solute-solvent attractive potential energy in water and a-seawater– may cause deviation from Setchenow relationship.

The following two references will be cited both in the manuscript and in *Supporting Information*.

Graziano, G.: Case study of enthalpy–entropy noncompensation. Journal of Chemical Physics, 120, 4467-4471, doi: 10.1063/1.1644094, 2004.

Graziano, G.: Salting out of methane by sodium chloride: A scaled particle theory study. Journal of Chemical Physics, 129, 084506, doi: 10.1063/1.2972979, 2008.

R2-6 ----------

(1) comments from Referee 2

The discussion in Sect. 3.3 assumes solubility equilibrium with the atmosphere over the full depth of the ocean mixed layer. How deep is this mixed ocean layer in the model? Does this mean the model estimates an upper limit?

(2) author's response

Thank you for the comments. The depth of the ocean mix layer in the model is 10 to 600 m. The depth distribution of CH_2F_2 dissolved in the ocean mixed layer in each semi-hemisphere is listed in Tables S4 (30° S–90° S), S5 (30° S–0° S), S6 (0° N–30° S) and S7 (30° N–90° N) in the revised manuscript. As seen in these tables, the CH_2F_2 dissolved in the ocean mixed layer resides mostly in less than 300 m depth. For example, for the southern semi-hemisphere (30° S–90° S) (Table S4), in August, when the amount of CH_2F_2 dissolved in the ocean mixed layer is maximum, 66% of the CH_2F_2 dissolved in the mixed layer would reside between 100 m and 200 m depth, and 91 % of the CH_2F_2 dissolved in the ocean mixed layer is expected to reside in less than 300 m depth.

As Referee 2 pointed out, model estimates mean an upper limit of the amount of CH_2F_2 dissolved in the ocean mixed layer. This point will be clearly described in the revised manuscript.

(3) author's changes in manuscript

lines 1-15, page 12:

As seen in Figure 6, in the southern semi-hemispheric lower troposphere (30° S–90° S), at least 5 % of the atmospheric burden of CH_2F_2 would reside in the ocean mixed layer in the winter, and the annual variance of the CH_2F_2 residence ratio would be 4%. These ratios are, in fact, upper limits because CH_2F_2 in the ocean mixed layer may be undersaturated. It takes days to a few weeks after a change in temperature or salinity for oceanic surface mixed layers to come to equilibrium with

the present atmosphere, and equilibration time increases with depth of the surface mixed layer (Fine, 2011). In the estimation using the gridded data here, >90 % of CH_2F_2 in the ocean mixed layer would reside in less than 300 m depth (Tables S3, S4, S5 and S6).

Haine and Richards (1995) demonstrated that seasonal variation in ocean mixed layer depth was the key process which affected undersaturation and supersaturation of chlorofluorocarbon 11 (CFC-11), CFC-12 and CFC-113 by use of a one-dimensional slab mixed model. As described above, >90 % of CH_2F_2 in the ocean mixed layer is expected to reside in less than 300 m depth. According to the model calculation results by Haine and Richards (1995), saturation of CH_2F_2 would be >0.9 for the ocean mixed layer with less than 300 m depth. The saturation of CH_2F_2 in the ocean mixed layer is thus estimated to be at least 0.8. In the southern semi-hemispheric lower troposphere (30° S–90° S), therefore, at least 4 % of the atmospheric burden of CH_2F_2 would reside in the ocean mixed layer in the winter, and the annual variance of the CH_2F_2 residence ratio would be 3%..

The following two references will be cited in the manuscript.

Fine, R. A.: Observations of CFCs and SF_6 as ocean tracers. Annual Review of Marine Science, 3, 173-195, doi:10.1146/annurev.marine.010908.163933, 2011.

Haine, T. W. N. and Richards, K. J.: The influence of the seasonal mixed layer on oceanic uptake of CFCs. Journal of Geophysical Research, 100, 10727-10744, doi:10.1029/95JC00629, 1995.

Supporting Information, Tables S4, S5, S6 and S7

Table S4. Monthly amount of CH_2F_2 dissolved in the ocean mixed layer at solubility equilibrium with the atmospheric CH_2F_2 (partial pressure, 1 patm) and the depth distribution of the CH_2F_2 dissolved in the southern semi-hemisphere (90°S - 30°S).

	Amount (Gg patm^{-1})	Depth distribution of CH_2F_2 dissolved in the ocean mixed layer (%)					
		10 - 100 m	100 - 200 m	200 - 300 m	300 - 400 m	400 - 500 m	500 - 600 m
January	0.0169	94.9	2.9	1.0	0.5	0.3	0.3
February	0.0201	92.1	3.6	2.9	1.0	0.3	0.0
March	0.0255	87.8	9.2	1.7	0.7	0.2	0.4
April	0.0338	66.5	31.8	1.1	0.2	0.1	0.2
May	0.0409	48.5	48.1	2.2	0.8	0.3	0.0
June	0.0510	26.8	62.7	8.0	1.7	0.8	0.1
July	0.0571	14.1	69.3	12.2	3.3	0.9	0.1
August	0.0640	8.5	65.8	17.0	6.2	2.3	0.2
September	0.0609	13.5	61.0	14.6	8.2	2.7	0.0
October	0.0504	24.7	58.6	12.1	2.9	1.4	0.3
November	0.0335	60.4	30.5	4.6	2.2	2.3	0.1
December	0.0196	95.1	4.3	0.4	0.2	0.0	0.0

Table S5. Monthly amount of CH_2F_2 dissolved in the ocean mixed layer at solubility equilibrium with the atmospheric CH_2F_2 (partial pressure, 1 patm) and the depth distribution of the CH_2F_2 dissolved in the southern semi-hemisphere (30°S - 0°S).

	Amount (Gg patm^{-1})	Depth distribution of CH_2F_2 dissolved in the ocean mixed layer (%)					
		10 - 100 m	100 - 200 m	200 - 300 m	300 - 400 m	400 - 500 m	500 - 600 m
January	0.0084	99.6	0.4	0	0	0	0
February	0.0084	99.7	0.3	0	0	0	0
March	0.0089	100.0	0	0	0	0	0
April	0.0106	100.0	0	0	0	0	0
May	0.0131	100.0	0	0	0	0	0
June	0.0163	97.1	2.9	0	0	0	0
July	0.0189	80.1	19.9	0	0	0	0
August	0.0193	73.1	26.9	0	0	0	0
September	0.0165	82.2	17.8	0	0	0	0
October	0.0124	94.6	5.4	0	0	0	0
November	0.0097	99.9	0.1	0	0	0	0
December	0.0087	100.0	0	0	0	0	0

Table S6. Monthly amount of CH_2F_2 dissolved in the ocean mixed layer at solubility equilibrium with the atmospheric CH_2F_2 (partial pressure, 1 patm) and the depth distribution of the CH_2F_2 dissolved in the southern semi-hemisphere (0°N - 30°N).

	Amount (Gg patm^{-1})	Depth distribution of CH_2F_2 dissolved in the ocean mixed layer (%)					
		10 - 100 m	100 - 200 m	200 - 300 m	300 - 400 m	400 - 500 m	500 - 600 m
January	0.0132	96.4	3.6	0	0	0	0
February	0.0126	95.9	4.1	0	0	0	0
March	0.0107	98.7	1.3	0	0	0	0
April	0.0087	99.8	0.2	0	0	0	0
May	0.0079	100.0	0	0	0	0	0
June	0.0080	100.0	0	0	0	0	0
July	0.0084	100.0	0	0	0	0	0
August	0.0082	100.0	0	0	0	0	0
September	0.0080	100.0	0	0	0	0	0
October	0.0086	100.0	0	0	0	0	0
November	0.0100	100.0	0	0	0	0	0
December	0.0118	100.0	0	0	0	0	0

Table S7. Monthly amount of CH_2F_2 dissolved in the ocean mixed layer at solubility equilibrium with the atmospheric CH_2F_2 (partial pressure, 1 patm) and the depth distribution of the CH_2F_2 dissolved in the southern semi-hemisphere (30°N - 90°N).

	Amount (Gg patm^{-1})	Depth distribution of CH_2F_2 dissolved in the ocean mixed layer (%)					
		10 - 100 m	100 - 200 m	200 - 300 m	300 - 400 m	400 - 500 m	500 - 600 m
January	0.0205	41.3	50.1	7.0	1.4	0.2	0.0
February	0.0225	34.5	55.3	7.1	2.3	0.6	0.2
March	0.0208	49.7	42.3	4.9	1.7	0.7	0.6
April	0.0147	79.7	17.6	1.7	0.4	0.0	0.6
May	0.0081	90.1	9.9	0	0	0	0
June	0.0055	97.7	2.3	0	0	0	0
July	0.0045	96.6	3.4	0	0	0	0
August	0.0048	94.4	5.6	0	0	0	0
September	0.0059	97.7	2.3	0	0	0	0
October	0.0084	99.6	0.4	0	0	0	0
November	0.0121	89.6	10.4	0.1	0	0	0
December	0.0163	71.0	26.1	2.9	0	0	0

R2-7 ----------

(1) comments from Referee 2

The conclusion that 5% of the atmospheric burden of CH_2F_2 would reside in the ocean mixed layer in the southern semi-hemispheric lower troposphere during winter seems to be an upper limit, and should be worded as such. How much lower could this upper limit be?

(2) author's response

Thank you for the comments. As described in R2-6, it takes days to a few weeks after a change in temperature or salinity for oceanic surface mixed layers to come to equilibrium with the present atmosphere, and equilibration time increases with depth of the surface mixed layer (Fine, 2011).

Haine and Richards (1995) demonstrated that the seasonal variation in ocean mixed layer depth was the key process which affected undersaturation and supersaturation of chlorofluorocarbon 11 (CFC-11), CFC-12 and CFC-113 by use of a one-dimensional slab mixed model. Specifically, the mixed layer deepening in autumn would cause undersaturation in the mixed layer. In the estimation, >90 % of CH_2F_2 in the ocean mixed layer is expected to reside in less than 300 m depth (Tables S3, S4, S5 and S6). According to the report by Haine and Richards (1995), saturation of CH_2F_2 would be >0.9 for the ocean mixed layer with less than 300 m depth. The saturation of CH_2F_2 in the ocean mixed layer is thus estimated to be at least 0.8.

The manuscript will be revised, as described in R6, and Fine (2011) and Haine and Richards (1995) will be

cited.

(3) author's changes in manuscript

lines 13-16, page 1, Abstract

By using this equation in a lower tropospheric semi-hemisphere (30° S–90° S) of the Advanced Global Atmospheric Gases Experiment (AGAGE) 12-box model, we estimated that 1 to 4 % of the atmospheric burden of CH_2F_2 resided in the ocean mixed layer and that this percentage was at least 4 % in the winter; dissolution of CH_2F_2 in the ocean may partially influence estimates of CH_2F_2 emissions from long-term observational data of atmospheric CH_2F_2 concentrations.

lines 20-24, page 12

By using the solubility of CH_2F_2 determined in this study, the magnitude of buffering of the atmospheric burden of CH_2F_2 by the additional CH_2F_2 in ocean surface waters is estimated to be realistically limited to only about 1 % globally; however, in a southern semi-hemispheric lower troposphere (30° S–90° S) of the AGAGE 12-box model, the atmospheric burden of CH_2F_2 is estimated to reside in the ocean mixed layer by at least 4 % in the winter and by 1 % in the summer.

Other changes are included in the change mentioned in R2-6.

R2-8 ----------

(1) comments from Referee 2

It seems surprising that the dissolution of CH_2F_2 into the ocean should affect estimates of CH_2F_2 emissions in the Southern Hemisphere and their seasonal variability, because the atmospheric concentrations that reach the Southern Hemisphere are also affected by transport, and chemical removal, and related uncertainties. This should be mentioned.

(2) author's response

Thank you for the comment. As Referee 2 pointed out, the atmospheric concentrations that reach the Southern Hemisphere are also affected by transport, chemical removal, and related uncertainties; this should be mentioned.

I will first describe how the dissolution of CH_2F_2 into the ocean may affect estimation of CH_2F_2 emissions in the Southern Hemisphere and their seasonal variability, and then I will show the revised text.

In 2012, atmospheric concentrations of CH_2F_2 in the Northern Hemisphere are by >30% higher than in the Southern Hemisphere (O'Doherty et al., 2014); the strong inter-hemisphere gradient indicates that emissions of CH_2F_2 are predominantly in the Northern Hemisphere. In the AGAGE 12 box model (Rigby et al., 2013), transport of CH_2F_2 is dominated by eddy diffusion between the boxes in the model. The seasonal eddy diffusion parameters between the Northern Hemisphere and the Southern Hemisphere in the model are 187 to 568 days in

lower troposphere, and 81 to 109 days in upper troposphere (Rigby et al., 2013).

The rate of increase in atmospheric concentration of CH_2F_2 due to the emission of CH_2F_2 in the Southern Hemisphere, which is denoted as RE_{south} hereafter, is thus more sensitive to change in atmospheric concentrations of CH_2F_2 in the Southern Hemisphere than those in the Northern Hemisphere, partly because CH_2F_2 is removed through gas phase reactions with OH (partial atmospheric lifetime of 5.5 years). Furthermore, RE_{south} would range small values such as a few % y^{-1} or less because emissions of CH_2F_2 were predominantly in the Northern Hemisphere and because, in 2012, the rate of increase in the global mean mole fraction of CH_2F_2 was 17% y^{-1} (O'Doherty et al., 2014). In estimation of RE_{south}, small value of RE_{south} would be deduced from difference in the rates of increase of atmospheric concentrations of CH_2F_2 between hemispheres. Dissolution of CH_2F_2 in the ocean in the Southern Hemisphere may thus affect estimation of RE_{south} and then affect estimation of CH_2F_2 emissions in the Southern Hemisphere and their seasonal variability.

I revise the text as follows.

(3) author's changes in manuscript

lines 5-10, page 12

In the Southern Hemisphere, CH_2F_2 emission rates are much lower than in the Northern Hemisphere. Hence, dissolution of CH_2F_2 in the ocean, even if dissolution is reversible, may influence estimates of CH_2F_2 emissions derived from long-term observational data on atmospheric concentrations of CH_2F_2; in particular, consideration of dissolution of CH_2F_2 in the ocean may affect estimates of CH_2F_2 emissions in the Southern Hemisphere and their seasonal variability because of slow rates of inter-hemispheric transport and small portion of the CH_2F_2 emissions in the Southern Hemisphere to the total emissions.

R2-9 ----------

(1) comments from Referee 2

On line 27, page 2 (in the revised manuscript), 'first' is written twice..

(2) author's response

Thank you for the comment. The text is revised.

(3) author's changes in manuscript

line 27, page 2

First, the values of K_H for CH_2F_2 were determined over the temperature range from 276 to 313 K by means of an inert-gas stripping (IGS) method.

R2-10----------

(1) comments from Referee 2

On lines 9-10, page 5 (in the revised manuscript), add errors for numbers. See comments #1, #2 and add typical values, their units, and uncertainties of variables for the key equations throughout the manuscript.

(2) author's response

Thank you for the comment. If redistribution of CH_2F_2 in the headspace to the test solution had occurred, the K_H values determined in this study would be overestimated. Errors due to this redistribution are always negative values. The ratio of the errors to the K_{eq} values (%) is $100 \times \frac{\left(\frac{V_{head}}{RTV}\right)}{\left(\frac{1}{k_1}\frac{F}{RTV}\right)}$, that is, $\frac{100k_1V_{head}}{F}$. Under the experimental conditions here, this ratio is calculated to be −2.0 to −2.3 % at 3.0 °C and −4.6 to −5.1 % at 39.5 °C. Values of this ratio increase as values of K_{eq} decrease. This ratio is maximum (−6.5 %) for a-seawater at 51.534‰ and 39.5 °C.

Typical values, their units, and uncertainties of variables for the key equations are added in the revised manuscript.

(3) author's changes in manuscript

lines 6-8, page 4

The solution was magnetically stirred, and its temperature was kept constant within ±0.2 K by means of a constant-temperature bath that had both heating and cooling capabilities (NCB-2500, EYELA, Tokyo, Japan) and was connected to the water jacket of the column.

lines 14-16, page 4

The volumetric flow rate of the gas (F_{meas}) was calibrated with a soap-bubble meter for each experimental run. The soap-bubble meter had been calibrated by means of a high-precision film flow meter SF-1U with VP-2U (Horiba, Kyoto, Japan). Errors of F_{meas} are within ±1%.

lines 19-20, page 4

All volumetric gas flows were corrected to prevailing temperature and pressure by Eq. (3) (Krummen et al., 2000). Errors due to this correction are within ±1%. Errors of F are thus within ±1.4%.

lines 14-21, page 5

Hence Eq. (6) was used to deduce $K_{eq}(T)$ from k_1. Errors of T are estimated to be within ±0.2 K. These errors of T may give potential systematic bias of ca. ±2% ($\delta K_{eq}/K_{eq}$) where δK_{eq} is error of the value of K_{eq}. Errors of F are estimated to be less

than 1.4 %, and these errors may give potential systematic bias of less than 1.4 % ($\delta K_{eq}/K_{eq}$). Accordingly, for the IGS methods, values of K_{eq} may have potential systematic bias of ca. ±2%.

If redistribution of CH_2F_2 in the headspace to the test solution had occurred, the values determined using Eq. (6) would be overestimated. Errors due to this redistribution are always negative values. Ratio of the errors to the K_{eq} values (%) is $\frac{100k_1V_{head}}{F}$. Values of this ratio increase as values of K_{eq} decrease. Under the experimental conditions here, this ratio is calculated to be from –2.0 % for water at 3.0 °C to −6.5 % for a-seawater at 51.534‰ and 39.5 °C.

lines 10-12, page 8

$$\ln(K_H(T)) = -49.71 + 77.70 \times \left(\frac{100}{T}\right) + 19.14 \times \ln\left(\frac{T}{100}\right) \quad (13)$$

The square-root-of-variance, that is, standard deviation for each fitting coefficient in Eq. (12) is as follows:

$\delta a_1 = 5.5$; $\delta a_2 = 8.3$; $\delta a_3 = 2.8$.

line 27, page 9 - line 1, page 11

This result suggests that $\ln(K_H(T)/K_{eq}{}^S(T))$ varied according to Eq. (18):

$$\ln\left(K_H(T)/K_{eq}{}^S(T)\right) = k_{s1} \times S^{0.5} \quad (18)$$

Values of k_{s1} may be represented by the following function of T:

$$k_{s1} = b_1 + b_2 \times \left(\frac{100}{T}\right) \quad (19)$$

Parameterizations of b_1 and b_2 obtained by fitting all the $\ln(K_H(T)/K_{eq}{}^S(T))$ and S data at each temperature simultaneously by means of the nonlinear least-squares method gives Eq. (20).

$$\ln\left(K_H(T)/K_{eq}{}^S(T)\right) = \left(0.0127 + 0.0099 \times \left(\frac{100}{T}\right)\right) \times S^{0.5} \quad (20)$$

The standard deviation for each fitting coefficient in Eq. (19) is as follows:

$\delta b_1 = 0.0106$; $\delta b_2 = 0.0031$.

Since $2\times\delta b_1 > b_1$, the parameterization by Eq. (19) may be overworked. Accordingly, all the $\ln(K_H(T)/K_{eq}{}^S(T))$ and S data at each temperature are fitted simultaneously using Eq. (21) instead of Eq. (19). The nonlinear least-squares method gives Eq. (22).

$$k_{s1} = b_2 \times \left(\frac{100}{T}\right) \quad (21)$$

$$\ln\left(K_H(T)/K_{eq}{}^S(T)\right) = 0.1343 \times \left(\frac{100}{T}\right) \times S^{0.5} \quad (22)$$

The standard deviation for the fitting coefficient in Eq. (21) is as follows: $\delta b_2 = 0.0013$. As seen in Fig. 5, Eqs. (21) and (22) reproduced the data well.

$\ln(K_H(T)/K_{eq}{}^S(T))$ depends on $S^{0.5}$ and follows Eq. (22) rather than the Setchenow dependence (Eq. (17)). Table S7 compares values of $K_{eq}{}^S$ calculated by Eq. (22) with those by Eq. (17). The difference between these values of $K_{eq}{}^S$ at 35‰ of

salinity was within 3% of the K_{eq}^{S} value. Decreases in values of K_{eq}^{S} are calculated to be 7–8% and 4%, respectively, by Eqs. (17) and (23) as salinity of a-seawater increases from 30‰ to 40‰ at each temperature.

The reason for this salting-out effect of CH_2F_2 solubility in a-seawater is not clear. Specific properties of CH_2F_2 –small molecular volume, which results in small work of cavity creation (Graziano, 2004; 2008), and large solute-solvent attractive potential energy in water and a-seawater– may cause deviation from Setchenow relationship (*Supporting Information*).

In Eq. (22), $K_H(T)$ is represented by Eq. (13), as described in Sect. 3.1. Therefore $K_{eq}^{S}(T)$ is represented by Eq. (23):.

$$\ln\left(K_{eq}^{S}\right) = -49.71 + (77.70 - 0.1343 \times S^{0.5}) \times \left(\frac{100}{T}\right) + 19.14 \times \ln\left(\frac{T}{100}\right) \quad (23)$$

The values calculated with Eq. (23) are indicated by the bold curves in Fig. 4 and are listed in Table 3. Table 3 lists errors at 95% confidence level for the regression. These errors ($error_{23}$) are calculated by Eq. (24):

$$error_{23} = K_{eq}^{S} \times \sqrt{\left(\frac{error_{13}}{K_H}\right)^2 + \left(\frac{error_{22}}{K_{eq}^{S}}\right)^2} \quad (24)$$

where $error_{13}$ represents errors at 95% confidence level for the regression by Eq. (12); $error_{22}$ represents errors at 95% confidence level for the regression by Eq. (21). Table 3 also represents errors due to both errors at 95% confidence level for the regression and potential systematic bias (±2%). Equation (23) reproduced the experimentally determined values of $K_H(T)$ and $K_{eq}^{S}(T)$ within the uncertainty of these experimental runs.

R2-11----------

(1) comments from Referee 2

What statistical test for outliers was applied? How many points were removed at each temperature?

(2) author's response

Thank you for the comment. Statistical test for outliers is as follows.

The data with errors being >10% of the data was first excluded. Next, some data were excluded for calculation of the average so that the remaining data were inside the 2σ range. This procedure was iterated until all the data were inside the 2σ range.

The number of them were eight or fewer at each temperature. The maximum number of the data excluded was corrected to be eight although it was described to be six in the original manuscript. Number of the data thus excluded were indicated in Tables 1 and 3 (R1-1).

(3) author's changes in manuscript

lines 19-22, page 7

The data with errors being >10% of the data was first excluded. Next, some data were excluded for calculation of the

average so that the remaining data were inside the 2σ range. This procedure was iterated until all the data were inside the 2σ range. The data points thus excluded was only for V values of 0.350 dm^3 and the number of them were eight or fewer at each temperature.

Tables 1 and 3

These tables in the revised manuscript are shown in R1-1.

R2-12----------

(1) comments from Referee 2

About Eq (17), for sake of discussion, can a k_S value be given here? And what is the effect of including k_S vs k_{S1}, k_{S2} in the model - does it make a difference?

(2) author's response

Thank you for the comment. Parameters of k_{S1}, k_{S2} in the original manuscript are replaced by a parameter of k_{S1} in the revised manuscript. I add Table S2. Table S2 lists values of k_s and comparison of the K_{eq} values calculated between by Eq. (17) and by Eq. (22) at salinity of 30, 35 and 40 ‰ and each temperature.

(3) author's changes in manuscript

lines 24-27, page 9

Figure 5 plots $\ln(K_H(T)/K_{eq}^S(T))$ against S at each temperature. Table S7 lists values of k_s determined by fitting the data at each temperature by use of Eq. (17). If the $K_{eq}^S(T)$ values obeyed Eq. (17), the data at each temperature in Fig. 5 would fall on a straight line passing through the origin, but they did not. Figure 5 reveals that the salinity dependence of CH_2F_2 solubility in a-seawater cannot be represented by Eq. (17).

lines 14-17, page 10

$\ln(K_H(T)/K_{eq}^S(T))$ depends on $S^{0.5}$ and follows Eq. (22) rather than the Setchenow equation (Eq. (17)). Table S14m lists ratios of K_{eq}^S calculated by Eq. (17) to those by Eq. (22). Difference between values of K_{eq}^S calculated by Eqs. (17) and (22) at 35‰ of salinity was within 3% of the K_{eq}^S value. Decreases in values of K_{eq}^S are calculated to be 7–8% and 4%, respectively, by Eqs. (17) and (23) as salinity of a-seawater increases from 30‰ to 40‰ at each temperature.

Table S2

Table S2. Values of k_s (Eq. (17)) and comparison of values of K_{eq}^{S} calculated at each temperature by Eq. (17) with those by Eq. (22).

Temperature (°C)	k_S (‰$^{-1}$)	[K_{eq}^{S} from Eq. (17)]/ [K_{eq}^{S} from Eq. (22)] at 30‰	at 35‰	at 40‰	[K_{eq}^{S} at 30‰]/ [K_{eq}^{S} at 40‰] Eq. (17)	Eq. (23)
3.0	0.00811	1.027	1.008	0.988	1.084	1.043
5.8	0.00785	1.033	1.014	0.995	1.082	1.042
10.5	0.00768	1.033	1.016	0.997	1.080	1.042
15.5	0.00718	1.044	1.028	1.012	1.074	1.041
20.3	0.00728	1.037	1.020	1.003	1.076	1.040
25.0	0.00704	1.040	1.024	1.008	1.073	1.039
29.9	0.00731	1.027	1.010	0.992	1.076	1.039
34.8	0.00713	1.029	1.012	0.995	1.074	1.038
39.5	0.00709	1.026	1.010	0.992	1.073	1.038